

High mobility InN epilayers grown on AlN epilayer templates

N. Khan, A. Sedhain, J. Li, J. Y. Lin, and H. X. Jiang^{a)}

Department of Physics, Kansas State University, Manhattan, Kansas 66506-2601, USA

(Received 3 April 2008; accepted 8 April 2008; published online 28 April 2008)

We report on the growth of InN epilayers on AlN/sapphire templates by metal organic chemical vapor deposition. Compared to InN epilayers grown on GaN templates, significant improvements in the electrical and optical properties of InN epilayers on AlN templates were observed. An increase in electron mobility, a decrease in background electron concentration, and a redshift of photoluminescence emission peak position with increasing the growth temperature and V/III ratio were observed and a room temperature Hall mobility of $1400 \text{ cm}^2/\text{V s}$ with a free electron concentration of about $7 \times 10^{18} \text{ cm}^{-3}$ was obtained. The improvements were partly attributed to the use of AlN templates, which allows for higher growth temperatures leading to an enhanced supply of nitrogen atoms and a possible reduction in the incorporation of unintentional impurities and nitrogen vacancy related defects. © 2008 American Institute of Physics. [DOI: 10.1063/1.2917473]

Among group III nitrides, InN has the narrowest direct band gap, the smallest electron effective mass, and the highest mobility and drift velocity.^{1,2} These distinctive properties make InN an interesting material for applications in full color displays and high frequency/high speed/high power electronic devices such as high electron mobility transistors (HEMTs).^{3,4} When alloyed with GaN, the energy band gap of InGaN can be tuned to cover the entire solar spectral region,⁵ which makes InGaN alloys highly promising for high efficiency multijunction solar cell applications. InGaN alloys could be potentially important thermoelectric materials for directly converting waste heat energy to electricity.⁶ In addition, the significant lattice mismatch between InN and GaN or AlN can result in a large piezoelectric charge, which may be advantageous for HEMT applications.⁷

As-grown unintentionally doped InN epilayers generally exhibit *n*-type conductivity, with unintentional free electron concentrations as high as 10^{21} cm^{-3} .⁸ Oxygen and hydrogen impurities are thought of as potential causes of the unintentional *n*-type conductivity in as-grown InN.^{9–11} On the other hand, the presence of nitrogen vacancies due to insufficient thermal decomposition of NH_3 at low growth temperatures ($\sim 500 \text{ }^\circ\text{C}$) has also been suggested as another major reason for the high background electron concentration in InN epilayers grown by metal organic chemical vapor deposition (MOCVD).^{8,12} More recently, it is widely accepted that InN films possess a surface electron accumulation layer due to the pinning of Fermi level at about 0.8 eV above the conduction band minimum due to intrinsic surface states.^{13–15} In general, due to the much lower dissociation temperature of InN than of GaN, it has been exceedingly difficult to grow InN epilayers with high quality by using the MOCVD method. As of today, InN epilayers with the highest material qualities are produced by molecular beam epitaxy.^{16,17} The highest room temperature electron mobility reported for MOCVD grown InN was about $1100 \text{ cm}^2/\text{V s}$ with an electron concentration of $\geq 10^{19} \text{ cm}^{-3}$ with the use of GaN/sapphire templates^{18,19} and it was found to be challenging to simultaneously enhance the electron mobility while reducing the background electron concentration.¹⁹ From a practical

point of view, there is a great need to develop and understand the growth processes to produce InN films with improved quality by MOCVD, which is currently the primary technique for producing all the commercially available III-nitride devices.

We report here on the MOCVD growth and transport and optical property studies of *c*-plane InN epilayers on *c*-plane AlN epilayer templates. There have not been many reports for InN epilayers grown on AlN templates, although it was pointed out that an InN/AlN heterojunction structure may provide a platform for future InN device applications due to its potentially excellent structural and electronic properties as a consequence of the large band gap difference between InN and AlN.²⁰ Compared to InN epilayers grown on GaN/sapphire templates, the use of AlN/sapphire templates facilitates a straightforward electrical property characterization by conventional techniques such as Hall effect measurement due to the insulating nature of AlN. Furthermore, we found that the use of AlN templates allows InN to be grown at higher temperatures than in the case of GaN templates, which enhanced the supply of nitrogen atoms from NH_3 at higher growth temperatures.

The $0.8 \mu\text{m}$ thick undoped InN epilayers were grown in a custom built MOCVD on AlN- or GaN-epilayer/sapphire (0001) templates. More details on the growth conditions and structural properties of AlN/sapphire templates can be found in our previous publications.^{21,22} Trimethylindium (TMIn), trimethylgallium (TMAI), and NH_3 were used as In, Al, and N sources, respectively. N_2 was used as a carrier gas for InN epilayer growth. The optimal growth temperature (T_G) for InN epilayers deposited on GaN templates (InN/GaN) was found to be $510 \text{ }^\circ\text{C}$ and InN films were observed to decompose (or evaporate) as T_G was raised to above $510 \text{ }^\circ\text{C}$. By varying the growth conditions, the highest electron mobility (μ) of InN/GaN we attain was $\sim 1000 \text{ cm}^2/\text{V s}$ with an electron concentration (n) of $\sim 1.2 \times 10^{19} \text{ cm}^{-3}$. In contrast, the highest T_G employed for InN epilayers deposited on AlN templates (InN/AlN) was $\sim 570 \text{ }^\circ\text{C}$, above which evaporation of InN starts to occur.

Figure 1 shows the photoluminescence (PL) spectra of undoped InN epilayers grown on AlN templates (InN/AlN) when T_G was increased from 510 to $570 \text{ }^\circ\text{C}$. The band-to-

^{a)}Electronic mail: jiang@phys.ksu.edu.

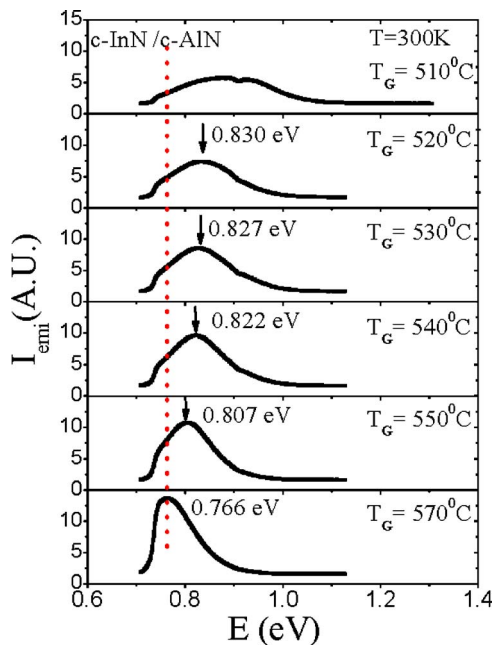


FIG. 1. (Color online) 300 K PL spectra of undoped InN epilayers grown on AlN templates (*c*-InN/*c*-AlN). The growth temperature (T_G) was varied from 510 to 570 °C.

band PL emission peak shifted from 0.87 to 0.76 eV as T_G was increased from 510 to 570 °C. Figure 2 summarizes the effects of T_G on the electrical and optical properties [integrated PL emission intensity (I_{emi}), PL emission peak position (E_p), background electron concentration (n), and mobility (μ)] of InN epilayers grown on AlN templates. Figures 2(a) and 2(b) show that I_{emi} increases, while E_p decreases as T_G was raised from 510 to 570 °C. Depicted in Figs. 2(c) and 2(d) are the plots of n and μ versus T_G . A decrease in n from 3.1 to $1.1 \times 10^{19} \text{ cm}^{-3}$ and an increase in μ from 690 to $1000 \text{ cm}^2/\text{V s}$ was observed as T_G was increased

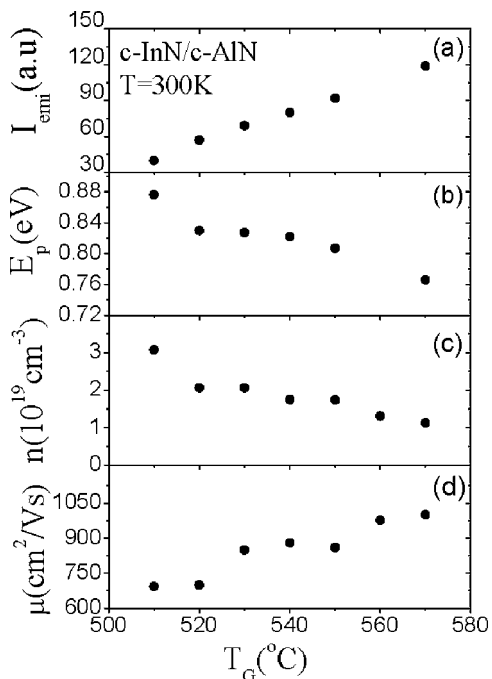


FIG. 2. Variations of (a) I_{emi} , (b) E_p , (c) n , and (d) μ of undoped InN grown on AlN template with the growth temperature (T_G).

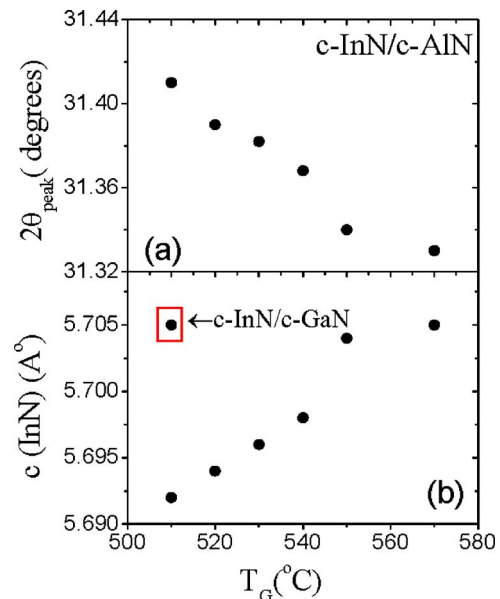


FIG. 3. (Color online) Variations of (a) XRD (θ - 2θ) scan peak position (b) calculated lattice constant c (InN) of undoped InN grown on AlN template with the growth temperature (T_G). Lattice constant c of InN grown on GaN template at 510 °C is also shown for comparison.

from 510 to 570 °C. The results are believed to be associated with an enhanced decomposition rate of NH_3 at higher T_G . An enhanced decomposition of NH_3 is likely to reduce the nitrogen vacancies and, henceforth, a decrease in the background electron concentration and an increase in mobility are observed.^{23,24} This observed decrease in n is consistent with the PL results shown in Figs. 1 and 2(a), where a redshift of E_p with T_G is clearly illustrated, attributing to a reduced Burstein–Moss blueshift due to a reduction in n .^{25–27} This attainment of higher growth temperature for the InN/AlN system may be related to the fact that the initial surface conditions for MOCVD growth are different from those of the InN/GaN system; however, a further understanding concerning the exact mechanisms is needed.

The x-ray diffraction (XRD) θ - 2θ scan results for InN grown on AlN are shown in Fig. 3. As illustrated in Fig. 3(a), (θ - 2θ) peak position for InN decreases from 31.41° to 31.33° as T_G increases from 510 to 570 °C. The InN lattice constant c , $c(\text{InN})$, deduced from the InN (0002) peak position is shown in Fig. 3(b), which shows that $c(\text{InN})$ increases from 5.690 to 5.705 Å as T_G increases from 510 to 570 °C. The measured value of $c(\text{InN})$ grown at 570 °C agrees well with a previously determined value of 5.704 Å.^{28,29} We also note that the lattice constant $c(\text{InN})$ grown on AlN template at 570 °C is the same as that of the InN grown on GaN template at 510 °C. The observed increase in $c(\text{InN})$ is related to an increase in compressive strain with increasing T_G . Concomitantly, InN lattice constant a , $a(\text{InN})$ is decreased with increasing T_G to compensate with the lattice constant of $a(\text{AlN})$. The full width at half maximum of the rocking curve of the (0002) peak of InN/AlN ranges from 700 to 1000 arc sec.

Further enhancement in the electrical properties of InN/AlN was obtained by increasing the V/III ratio during the growth. Figure 4 shows the dependence of the n and μ of InN on the V/III ratio for layers grown at 570 °C. It is seen that n decreases from 1.1×10^{19} to $6 \times 10^{18} \text{ cm}^{-3}$ and μ increases from ~ 1000 to $\sim 1400 \text{ cm}^2/\text{V s}$ as the V/III

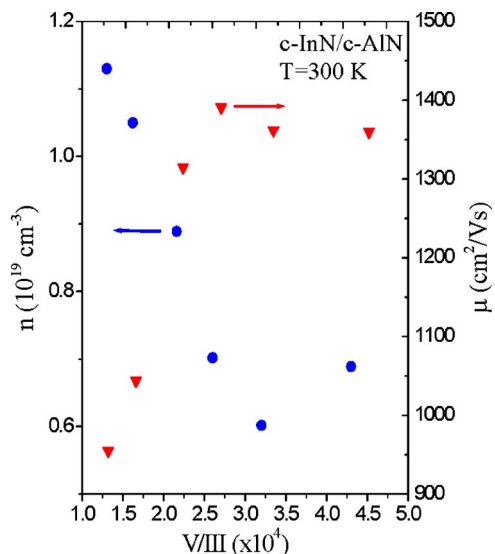


FIG. 4. (Color online) Free electron concentration (n) and mobility (μ) of undoped InN grown on AlN template as a function of the V/III ratio with a growth temperature of 570 °C. Indium flow rate was changed from 200 to 60 ml/min, which corresponds to a V/III ratio variation from 1.3×10^4 to 4.3×10^4 .

ratio is increased from 1.3×10^4 to 4.3×10^4 . This is the highest electron mobility ever reported for InN epilayers grown by MOCVD. The band-to-band emission peak position in samples with $n = (6-7) \times 10^{18} \text{ cm}^{-3}$ and $\mu = (1350-1400) \text{ cm}^2/\text{V s}$ is further reduced to $\sim 0.75 \text{ eV}$. Intuitively, the results shown in Fig. 4 seem to suggest that the reduction of n is associated with a decrease in nitrogen vacancies. However, the V/III ratio may also impact the incorporation of other unintentional impurities, such as hydrogen and oxygen.

In summary, the electrical and optical properties of InN epilayer deposited on AlN templates have been studied as functions of the MOCVD growth temperature and V/III ratio. A room temperature Hall mobility of $1400 \text{ cm}^2/\text{V s}$ with a carrier concentration of $7 \times 10^{18} \text{ cm}^{-3}$ was achieved, which represents the highest electron mobility value reported for MOCVD grown InN epilayers. The results suggested that the use of AlN templates could open up a new avenue for obtaining InN with reduced background electron concentrations and enhanced mobilities.

This work is supported by NSF (DMR-0504601) and AFOSR (FA9550-06-1-0441).

¹Y. Nanishi, Y. Saito, and T. Yamaguchi, *Jpn. J. Appl. Phys., Part 1* **42**,

2549 (2003).

²F. H. Yang, J. S. Hwang, Y.-J. Yang, K. H. Chen, and J. H. Wang, *Jpn. J. Appl. Phys., Part 2* **41**, L1321 (2002).

³B. E. Foutz, S. K. O'Leary, M. S. Shur, and L. F. Eastman, *J. Appl. Phys.* **85**, 7727 (1999).

⁴E. Bellotti, B. K. Doshi, K. F. Brennan, J. D. Albrecht, and P. P. Ruden, *J. Appl. Phys.* **85**, 916 (1999).

⁵J. Wu, W. Walukiewicz, K. M. Yu, W. Shan, W. J. Ager, E. E. Haller, H. Lu, W. J. Schaff, W. K. Mertzger, and S. Kurtz, *J. Appl. Phys.* **94**, 6477 (2003).

⁶B. N. Pantha, R. Dahal, J. Li, J. Y. Lin, H. X. Jiang, and G. Pomrenke, *Appl. Phys. Lett.* **92**, 042112 (2008).

⁷B. E. Foutz, O. Ambacher, M. J. Murphy, V. Tilak, and L. F. Eastman, *Phys. Status Solidi B* **216**, 415 (1999).

⁸A. G. Bhuiyan, A. Hashimoto, and A. Yamamoto, *J. Appl. Phys.* **94**, 2779 (2003).

⁹C. Stampfl, C. G. Van de Walle, D. Vogel, P. Kruger, and J. Pollmann, *Phys. Rev. B* **61**, R7846 (2000).

¹⁰D. C. Look, H. Lu, W. J. Schaff, J. Jasinski, and Z. Liliental-Weber, *Appl. Phys. Lett.* **80**, 258 (2002).

¹¹A. Janotti and C. G. Van de Walle, *Appl. Phys. Lett.* **92**, 032104 (2008).

¹²A. G. Bhuiyan, T. Tanaka, A. Yamamoto, and A. Hashimoto, *Phys. Status Solidi A* **194**, 502 (2002).

¹³H. Lu, W. J. Schaff, L. F. Eastman, and C. E. Stutz, *Appl. Phys. Lett.* **82**, 1736 (2003).

¹⁴I. Mahboob, T. D. Veal, C. F. MacConville, H. Lu, and W. J. Schaff, *Phys. Rev. Lett.* **92**, 036804 (2004).

¹⁵D. Segev and C. G. Van de Walle, *Europhys. Lett.* **76**, 305 (2006).

¹⁶H. Lu, W. J. Schaff, J. Hwang, H. Wu, and G. Koley, *Appl. Phys. Lett.* **79**, 1489 (2001).

¹⁷X. Wang, S. B. Che, Y. Ishitani, and A. Yoshikawa, *Appl. Phys. Lett.* **90**, 201913 (2007).

¹⁸C. A. Chang, C. F. Shih, N. C. Chen, P. Chang, and K. S. Liu, *Phys. Status Solidi C* **1**, 2559 (2004).

¹⁹A. Yamamoto, H. Miwa, Y. Shibata, and A. Hashimoto, *Phys. Status Solidi C* **3**, 1527 (2006).

²⁰C. L. Wu, C. H. Shen, and S. Gwo, *Appl. Phys. Lett.* **88**, 032105 (2006).

²¹M. Higashiwaki and T. Matsui, *J. Cryst. Growth* **252**, 128 (2003).

²²B. N. Pantha, R. Dahal, M. L. Nakarmi, N. Nepal, J. Li, J. Y. Lin, H. X. Jiang, Q. S. Paduano, and D. Weyburne, *Appl. Phys. Lett.* **90**, 241101 (2007).

²³B. N. Pantha, N. Nepal, T. M. Al Tahtamouni, M. L. Nakarmi, J. Li, J. Y. Lin, and H. X. Jiang, *Appl. Phys. Lett.* **91**, 121117 (2007).

²⁴A. Yamamoto, Y. Murakami, K. Koide, M. Adachi, and A. Hashimoto, *Phys. Status Solidi B* **228**, 5 (2001).

²⁵V. Y. Davydov, A. A. Klochikhin, V. V. Emtsev, S. V. Ivanov, V. V. Vekshin, F. Bechstedt, J. Furthmuller, H. Harima, A. V. Mudryi, A. Hashimoto, Y. Yamamoto, J. Aderhold, J. Graul, and E. E. Haller, *Phys. Status Solidi B* **230**, R4 (2002).

²⁶M. Higashiwaki, T. Inushima, and T. Matsui, *Phys. Status Solidi B* **240**, 417 (2003).

²⁷K. Sugita, H. Takasuka, A. Hashimoto, and A. Yamamoto, *Phys. Status Solidi B* **240**, 421 (2003).

²⁸V. Y. Davydov, A. A. Klochikhin, R. P. Seisyan, V. V. Emtsev, S. V. Ivanov, F. Bechstedt, J. Furthmuller, H. Harima, A. V. Mudryi, J. Aderhold, O. Semchinova, and J. Graul, *Phys. Status Solidi B* **229**, R1 (2002).

²⁹O. K. Semchinova, J. Aderhold, J. Graul, A. Filimonov, and H. Neff, *Appl. Phys. Lett.* **83**, 5440 (2003).